OPEN

Oncogene (2018) **37**, 439–449

www.nature.com/onc

ORIGINAL ARTICLE

Mobilan: a recombinant adenovirus carrying Toll-like receptor 5 self-activating cassette for cancer immunotherapy

V Mett[1,6], EA Komarova[2,6], K Greene[2], I Bespalov[1], C Brackett[2], B Gillard[3], AS Gleiberman[1], IA Toshkov[1], S Aygün-Sunar[1], C Johnson[2], E Karasik[3], M Bapardekar-Nair[1], OV Kurnasov[4], AL Osterman[4], PS Stanhope-Baker[1], C Morrison[5], MT Moser[3], BA Foster[3] and AV Gudkov[1,2]

Toll-like receptor 5 (TLR5) is considered an attractive target for anticancer immunotherapy. TLR5 agonists, bacterial flagellin and engineered flagellin derivatives, have been shown to have potent antitumor and metastasis-suppressive effects in multiple animal models and to be safe in both animals and humans. Anticancer efficacy of TLR5 agonists stems from TLR5-dependent activation of nuclear factor-κB (NF-κB) that mediates innate and adaptive antitumor immune responses. To extend application of TLR5-targeted anticancer immunotherapy to tumors that do not naturally express TLR5, we created an adenovirus-based vector for intratumor delivery, named Mobilan that drives expression of self-activating TLR5 signaling cassette comprising of human TLR5 and a secreted derivative of *Salmonella* flagellin structurally analogous to a clinical stage TLR5 agonist, entolimod. Co-expression of TLR5 receptor and agonist in Mobilan-infected cells established an autocrine/paracrine TLR5 signaling loop resulting in constitutive activation of NF-κB both *in vitro* and *in vivo*. Injection of Mobilan into primary tumors of the prostate cancer-prone transgenic adenocarcinoma of the mouse prostate (TRAMP) mice resulted in a strong induction of multiple genes involved in inflammatory responses and mobilization of innate immune cells into the tumors including neutrophils and NK cells and suppressed tumor progression. Intratumoral injection of Mobilan into subcutaneously growing syngeneic prostate tumors in immunocompetent hosts improved animal survival after surgical resection of the tumors, by suppression of tumor metastasis. In addition, vaccination of mice with irradiated Mobilan-transduced prostate tumor cells protected mice against subsequent tumor challenge. These results provide proof-of-concept for Mobilan as a tool for antitumor vaccination that directs TLR5-mediated immune response toward cancer cells and does not require identification of tumor antigens.

Oncogene (2018) **37,** 439–449; doi:10.1038/onc.2017.346; published online 2 October 2017

INTRODUCTION

Toll-like receptors (TLRs) are major regulators of innate and adaptive immunity and are gaining increasing attention as potential targets for preventing and treating cancer. In particular, pharmacological activation of TLR5 by its natural agonist flagellin or engineered agonists[1] has been shown to stimulate antitumor immune responses in multiple animal tumor models[2–7] and models of liver metastasis.[5,8–11] These therapeutic effects stem from ligand-induced TLR5 signaling leading to MyD88-dependent activation of nuclear factor-κB (NF-κB) and subsequent transcriptional induction of numerous genes related to inflammation and host defense.[12,13] Similar to agonists of other TLRs, flagellin activates innate immune cells that induce maturation and chemokine production in dendritic cells[14–16] and stimulates $CD4^+$ T cells to produce interferon-γ, interleukin (IL)-8 and IL-10, but not IL-4. These cytokines can promote a Th1-type response and are beneficial for generating efficient $CD8^+$ T-cell responses. It was found that antitumor activity of flagellin was associated with mobilization of different classes of immune cells, in particular, neutrophils and NK cells leading to stimulation of $CD8^+$T-cell responses.[6,9,10]

TLR5 agonists are promising anticancer agents because of their safety, as well as their efficacy. Unlike many other TLRs, TLR5 signaling, while immunostimulatory, does not induce certain highly pro-inflammatory cytokines that can cause a self-amplifying and potentially dangerous 'cytokine storm'.[17–19] The safety of TLR5 agonists is supported by the results of two clinical studies in which >150 healthy subjects and cancer patients were administered the flagellin derivative entolimod (previously CBLB502), which is being developed for tissue protective and anticancer applications (https://clinicaltrials.gov/ct2/show/NCT02654938).

Antitumor/metastatic efficacy of TLR5 agonists correlates not only with TLR5 expression by the tumor itself[3,4,6] but also with TLR5 expression in the tumor microenvironment (for example, suppression of liver metastasis of TLR5-negative tumors).[8] Here we introduce a strategy to increase the range of tumors that may be effectively treated via TLR5 agonist-dependent immunotherapy. An adenovirus-based construct (Mobilan-VM3 or M-VM3) was generated to direct co-expression of TLR5 and a secreted variant of entolimod with the expectation that delivery of the construct to a tumor would establish potent autocrine/paracrine TLR5 activation regardless of the tumor's natural TLR5 expression status. We hypothesized that Mobilan-driven TLR5 signaling within a tumor

[1]Cleveland Biolabs Inc., Buffalo, NY, USA; [2]Department of Cell Stress Biology, Roswell Park Cancer Institute, Buffalo, NY, USA; [3]Department of Molecular Pharmacology and Cancer Therapeutics, Roswell Park Cancer Institute, Buffalo, NY, USA; [4]Infectious and Inflammatory Disease Center, Sanford-Burnham-Prebys Medical Discovery Institute, La Jolla, CA, USA and [5]Department of Pathology, Roswell Park Cancer Institute, Buffalo, NY, USA. Correspondence: Dr AV Gudkov, Department of Cell Stress Biology, Roswell Park Cancer Institute, CGP L3-310, Elm and Carlton Streets, Buffalo, NY 14263, USA.
E-mail: andrei.gudkov@roswellpark.org
[6]These authors contributed equally to this work.
Received 26 April 2017; revised 23 July 2017; accepted 7 August 2017; published online 2 October 2017

would stimulate innate immune responses capable of suppressing primary tumor growth and also providing long-term protection against metastases and recurrent tumors.

To test this approach, we focused on prostate cancer after finding that most prostate cancers express the Coxsackie virus and adenovirus receptor (CAR)[20] required for efficient infection by serotype 5 adenovirus-based vectors such as Mobilan.

Prostate cancer is extremely common, with a 14% lifetime risk of diagnosis for American men, and remains the second leading cause of cancer death in this demographic group.[21] Therefore, development of new, more effective treatments for prostate cancer is critical. Our hypothesis that Mobilan may address this need is supported by the efficacy of several other immunotherapeutic approaches against prostate cancer. These include cell-based vaccines (Sipuleucel-T, BPX-101, DCVAC/Pa, GVAX),[21–26] virus-based vaccines (PROSTVAC-VF)[27,28] and antibodies against immune checkpoint proteins (CTLA-4, PD1/PD-L1).[29–36] However, none of these strategies were found to extend survival for more than a few months.

For our studies with Mobilan-VM3, we used the well-known transgenic adenocarcinoma of the mouse prostate (TRAMP) model,[37–39] which has been widely adopted to evaluate candidate therapies.[40–42] In this model, expression of the large and small SV40 tumor antigens from the prostate-specific rat probasin promoter leads to spontaneous development of epithelial hyperplasia in the prostate by 8 weeks of age and then to malignant adenocarcinomas.[43] Infection of TRAMP prostate tumor cells with M-VM3 established expression of both TLR5 and secreted entolimod as expected and induced activation of NF-κB *in vitro* and *in vivo*. Intraprostate tumor injections of M-VM3 in TRAMP mice led to strong induction of inflammatory genes, mobilization of innate immune cells into tumors and signs of tumor atrophy. Further support for use of Mobilan against prostate cancer was provided by results showing that intratumoral (i.t.) injection of M-VM3 into subcutaneous (s.c.) prostate tumors improved animal survival after surgical resection of the tumors (that is, suppressed tumor metastasis) and that vaccination of mice with irradiated M-VM3-infected prostate tumor cells protected mice against tumor challenge.

RESULTS

Generation and characterization of Mobilan vectors

In the very first variant of Mobilan, Mobilan-0 (M-0), a bi-cistronic expression cassette that directs constitutive expression of full-length human TLR5 from the cytomegalovirus promoter and a secreted version of the flagellin-based TLR5 agonist CBLB502 (CBLB502s)[44] from the EF1 promoter (Figure 1A(a)) was cloned into a non-replicating adenoviral vector (pDC515/ pBHGloxΔE1,3 Cre). Western blotting confirmed production of both hTLR5 and CBLB502 proteins by M-0-infected TLR5-negative MOSEC murine ovarian cancer cells (Figure 1B). However, CBLB502s produced in these cells had a larger apparent size on the blots than expected and its specific activity (ratio of CBLB502s amount measured by ELISA and its NF-κB-activating capacity in HEK293-NF-κB-lacZ reporter cells) was only ~1% of that observed for CBLB502 produced in *Escherichia coli*. The presence of four predicted glycosylation sites in the amino-acid sequence of CBLB502 suggested that CBLB502s produced in mammalian cells may be inactive because of glycosylation. Indeed, treatment of lysates of M-0-infected MOSEC cells with de-glycosylating enzymes resulted in a shift in the mobility of CBLB502s to the expected size (Figure 1B(b)). A 'non-glycosylated' mutant version of CBLB502 (CBLB502NQ) containing asparagine to glutamine substitutions in all four predicted glycosylation sites was produced in *E. coli* and found to have similar specific activity in HEK293-NF-κB-lacZ reporter cells to CBLB502 (Figure 1C). After generation and testing of a series of Mobilan versions with CBLB502NQ TLR5 agonist, an optimized adenoviral construct (named Mobilan-VM3 or M-VM3) was generated that expresses balanced levels of CBLB502NQs and hTLR5 from the UbiC promoter and cytomegalovirus promoter, respectively (Figure 1A(b)). Control adenoviral construct expressing red fluorescent protein mCherry was also generated (Figure 1A(c)). The specific activity of CBLB502NQs produced in M-VM3-infected MOSEC cells was similar to that of the *E. coli*-produced CBLB502 (Figure 1D); this was likely because of partial degradation of CBLB502NQs during expression (Figure 1E).

Establishment of fully functional autocrine/paracrine TLR5 signaling in the cells transduced with M-VM3 was demonstrated in TLR5-negative MOSEC cells (non-responsive to entolimod, Supplementary Figure S1) using nuclear translocation of the p65 subunit of NF-κB as an indicator of its activation (Figure 1F). M-VM3 infection also led to p65 nuclear localization in hepatocyte cultures from TLR5KO mice (Supplementary Figure S1). We also tested functionality of M-VM3 in the TRAMP-C2 prostate cancer cell line established from a primary TRAMP mouse prostate tumor.[37] TRAMP-C2 cells were stably transfected with an NF-κB reporter construct and then infected with M-VM3 or a control adenovirus directing cytomegalovirus promoter-driven red fluorescent protein expression (Ad-mCherry). Dose-dependent NF-κB activation was observed in the M-VM3-infected TRAMP-C2 cells (Figure 1G).

One potential limitation for clinical use of TLR5 agonists is pre-existence of a prohibitively high level of anti-flagellin neutralizing antibodies in ~10% of humans (CBLI, unpublished), likely because of exposure to flagellated enterobacteria of the gut microflora. However, we found that anti-flagellin neutralizing antibodies did not significantly affect M-VM3-directed TLR5 signaling in MOSEC-NF-κB-luciferase reporter cells (Figure 1H) even with antibody levels 10-fold higher than that required to neutralize CBLB502NQs added to the medium of TLR5-positive HEK293-NF-κB-lacZ reporter cells (Supplementary Figure S2). These results suggest that in M-VM3-infected cells, TLR5 interacts with CBLB502NQs during co-secretion and the complex is either inaccessible to or cannot be disrupted by neutralizing antibodies. Resistance of M-VM3-induced TLR5 signaling to neutralizing antibodies would allow its therapeutic use in a wider human population compared with entolimod.

The choice of tumor type for Mobilan application

Cell surface expression of the CAR is required for efficient infection of cells by vectors made on the basis of adenovirus serotype 5, such as M-VM3. To identify tumor types expressing CAR and, therefore, potentially transducible by M-VM3, we stained human tissue microarrays from the Roswell Park Cancer Institute (RPCI) Pathology Core with anti-CAR antibodies. Based on the analysis of a tissue microarray containing 252 samples (Supplementary Figure S3, Supplementary Table S3) representing 23 different tumor types and 12 different normal tissues, we divided tumor types into three categories: (i) low CAR expression (hematopoietic, soft tissue, skin, head and neck, brain, cervical, breast, and esophageal tumors); (ii) high CAR expression (bladder, prostate cancer, small intestine, thyroid, testicular and colon tumors); and (iii) mid-range CAR expression (lung, ovary, stomach, kidney, melanoma, liver, endocrine and mesothelioma tumors). We then focused on prostate tumors and analyzed CAR expression using tissue microarray containing 134 prostate cancer-derived and 134 normal prostate-derived samples. In all, 90% of all prostate samples (regardless of normal or cancerous) were found to be strongly CAR positive (Figure 2a). High CAR expression was also detected in TRAMP-C2 murine prostate cancer cells (Figure 2b). These observations suggest that M-VM3 treatment could be effective in the vast majority of prostate cancer patients, as well as in the prostate tumors in TRAMP mice.

To confirm the latter expectation, we injected Ad-mCherry (5×10^8 v.p./tumor) directly into TRAMP mouse prostate tumors

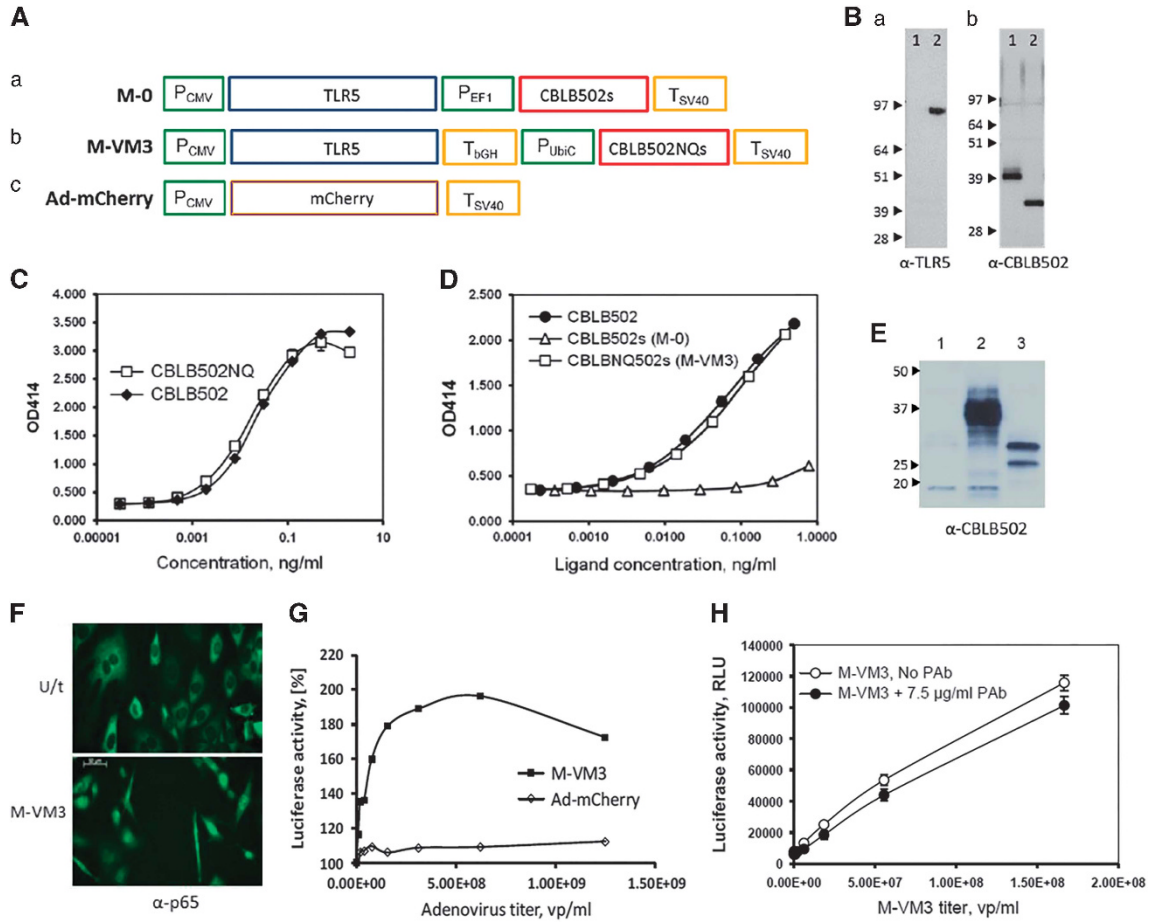

Figure 1. Adenoviral constructs and their characterization *in vitro*. (**A**) Schematic representation of expression cassettes in (a) Mobilan M-0, (b) Mobilan M-VM3, and (c) Ad-mCherry. P, promoter, T, transcription terminator. (**B**) Western blot analysis of Mobilan-directed protein expression in MOSEC cells. (a) Detection with anti-TLR5 antibody; lysates from uninfected (lane 1) and M-0-infected MOSEC cells (lane 2). (b) Detection with rabbit anti-CBLB502 pAb; lysates from M-0-infected MOSEC cells left untreated (lane 1) or treated with a mixture of deglycosylation enzymes (lane 2). (**C**) Activity comparison of *E. coli*-produced CBLB502 and CBLB502NQs in HEK293-NF-κB-lacZ reporter cells. Cells were incubated with purified proteins for 24 h; β-galactosidase activity (OD414) was measured in cell lysates using ONPG substrate. (**D**) Activity comparison of CBLB502s and CBLB502NQs produced in MOSEC cells. MOSEC cells were infected with M-0 or M-VM3, medium was collected after 48 h and the concentrations of CBLB502s and CBLB502NQs were measured by ELISA after heat-inactivation of residual adenovirus. The indicated amounts of MOSEC-produced proteins or *E. coli*-produced CBLB502 standard were applied to HEK293-NF-κB-lacZ cells and β-galactosidase was measured as above. (**E**) Western blot analysis of MOSEC cells infected with Ad-mCherry (lane 1), M-0 (lane 2) or M-VM3 (lane 3) using rabbit anti-CBLB502 pAb. The protein with slower mobility in lane 3 is the expected size of unglycosylated CBLB502NQs (31.5 kDa); the faster mobility protein is presumably a partially degraded form of CBLB502NQs. (**F**) Infection with M-VM3 (MOI = 3×10^4) induces NF-κB p65 nuclear translocation in TLR5-negative MOSEC cells 24 h after infection compared with control uninfected MOSEC cells. Antibodies against NF-κB p65 were used for immunostaining. (**G**) Induction of NF-κB-dependent luciferase expression in TRAMP-C2 cells infected by M-VM3. TRAMP-C2 cells carrying an NF-κB-dependent luciferase reporter construct were infected with M-VM3 or Ad-mCherry at the indicated MOIs. Luciferase activity was measured in lysates prepared 48 h post-infection and is shown as a percentage of that in uninfected cells (set at 100%). (**H**) Effect of neutralizing anti-CBLB502 antibodies on TLR5 signaling in M-VM3-infected MOSEC-NF-κB-luciferase reporter cells. Cells were infected with M-VM3 in the presence or absence of an excess of neutralizing rabbit anti-CBLB502 pAb. Luciferase activity was measured after 80-h incubation. Graphs show mean ± s.d. of triplicate measurements.

(Figure 2c) and surgical specimens of human prostate tumors (Figure 2d). In both cases, mCherry expression was observed in CAR-positive epithelial cells 24 h post-infection. This finding supports the likelihood of efficient M-VM3 infection of prostate tumors *in vivo*.

Mobilan induces constitutive activation of NF-κB in transduced cells

Self-activating TLR5 cassette transduced by Mobilan is expected to generate constitutive activity of the TLR5 pathway because of constant intrinsic stimulation by the interaction of co-expressed TLR5 and its ligand. We expected that the dynamic of M-VM3-driven TLR5-mediated activity will be different from that induced by stimulation with extrinsically applied TLR5 agonist, which is known to be transient because of TLR5 depletion and negative feedback mechanisms of NF-κB regulation. Cultures of mouse hepatocytes carrying an NF-κB-dependent luciferase reporter were either transduced with M-VM3 or treated with entolimod added to the medium and the activity of reporter was constantly monitored during 2 days using LumiCycle (Figure 3a). As expected, *in vitro* treatment of hepatocytes with entolimod resulted in rapid but transient NF-κB activation. In contrast, the dynamic of NF-κB activation in response to M-VM3 was slower but reached similar levels and stayed stably high during the whole observation period, thus demonstrating the desirable and planned activity of M-VM3.

To examine M-VM3 functionality in the whole-animal setting, we compared NF-κB activation in Balb/C-Tg(IκBα-luc)Xen NF-κB

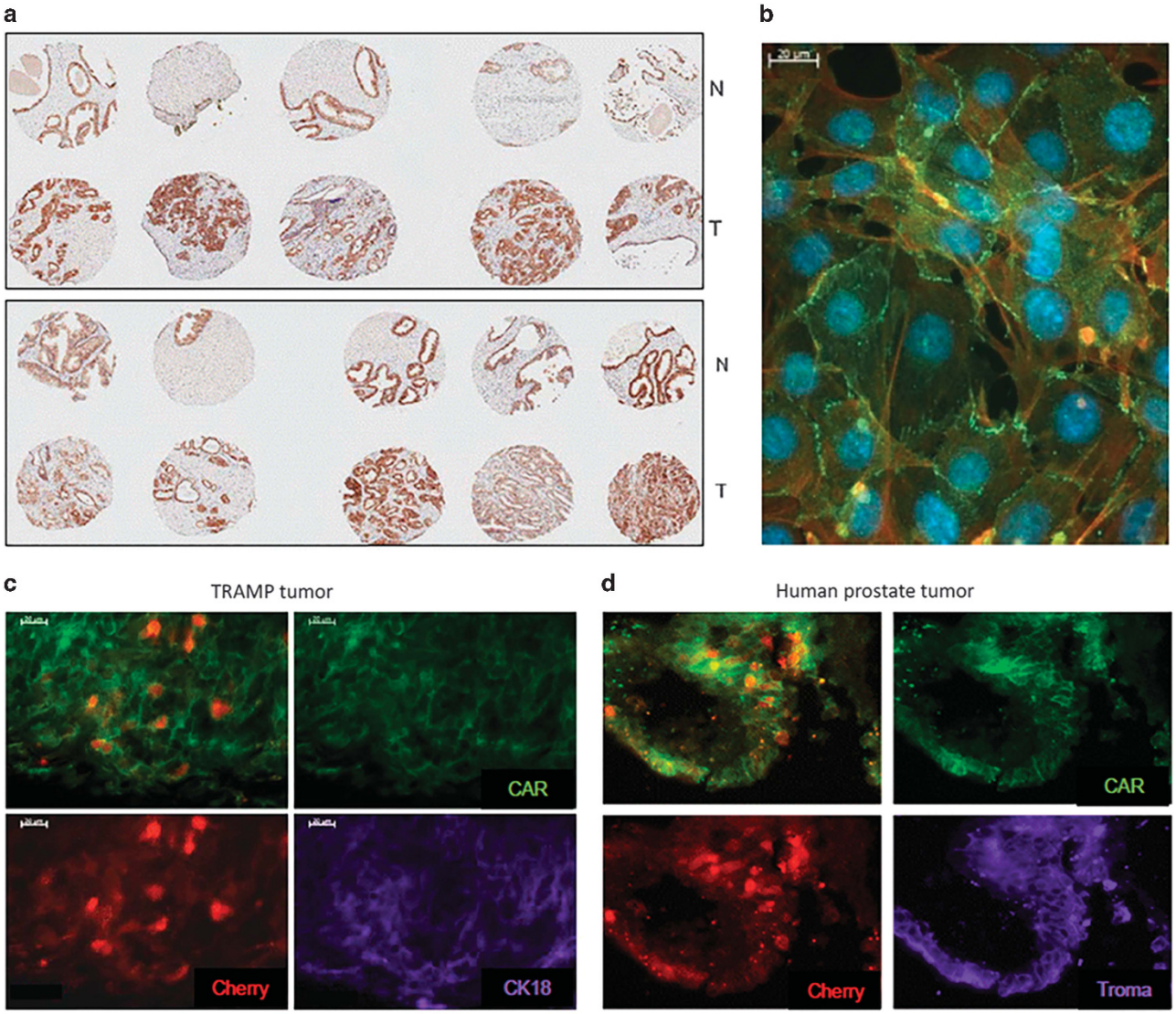

Figure 2. Mouse and human prostate tumors express CAR and are efficiently infected by Ad-mCherry. (**a**) A representative area of a human prostate tumor microarray (RPCI) stained with anti-CAR antibodies (T—tumor and N—normal prostate tissue samples). (**b**) Expression of CAR (green) in TRAMP-C2 cells revealed by immunofluorescent staining with anti-CAR antibodies. (**c**) A TRAMP mouse prostate tumor was injected with Ad-mCherry (5×10^8 v.p./tumor). Twenty-four hours later, CAR (green) and mCherry (red) expression were detected in tumor epithelial cells positive for CK8/18, a marker of epithelial cells (lilac). The upper left picture shows an overlay of CAR and mCherry fluorescence. (**d**) A human prostate tumor surgical sample (RPCI) was injected with AdCherry (5×10^8 v.p./tumor). Twenty-four hours later, CAR (green) and mCherry (red) expression was detected in tumor epithelial cells positive for Troma I, a marker of epithelial cells (lilac). The upper left picture shows an overlay of CAR and mCherry fluorescence.

reporter mice treated with M-VM3 or entolimod. Whole-body bioluminescence imaging of these mice at 3, 24 and 48 h after intraprostate injections showed that entolimod induced rapid NF-κB activation in the liver area (at 3 h), which diminished by 24 h. In contrast, M-VM3 activated NF-κB slowly in the lower abdominal area (at 24 h) and this persisted during the whole observation period (48 h) (Figure 3b). NF-κB-driven luciferase expression was measured in lysates of liver, intestine and prostate prepared from reporter mice 48 h after M-VM3 intravenous or intraprostate injections (Figure 3c). Intravenous M-VM3 resulted in strong NF-κB activation in the liver, lesser activation in the intestine, and no significant activation in the prostate. In contrast, intraprostate M-VM3 injection caused significant NF-κB activation in prostate tissue, some activation in intestine and no substantial activation in liver. These results show lack of systemic leakage of functional amounts of TLR5 agonist from the transduced site (what otherwise would be detected by NF-κB activation in the liver).

Our findings that M-VM3 is capable of establishing continuous TLR5 signaling in cultured cells, as well as in mice, particularly in prostate tissue provide proof-of-concept for the idea behind Mobilan and support the feasibility of using M-VM3 to treat prostate cancer.

Intraprostate M-VM3 injection in TRAMP mice leads to reduced organ weight and mobilization of immune cells into the hyperplastic prostate

The ability of M-VM3 to suppress prostate tumor progression in the TRAMP model was tested by administering M-VM3, Ad-mCherry or phosphate-buffered saline (PBS) to 12-week-old mice by intraprostate injection. Six weeks later, mice were evaluated for

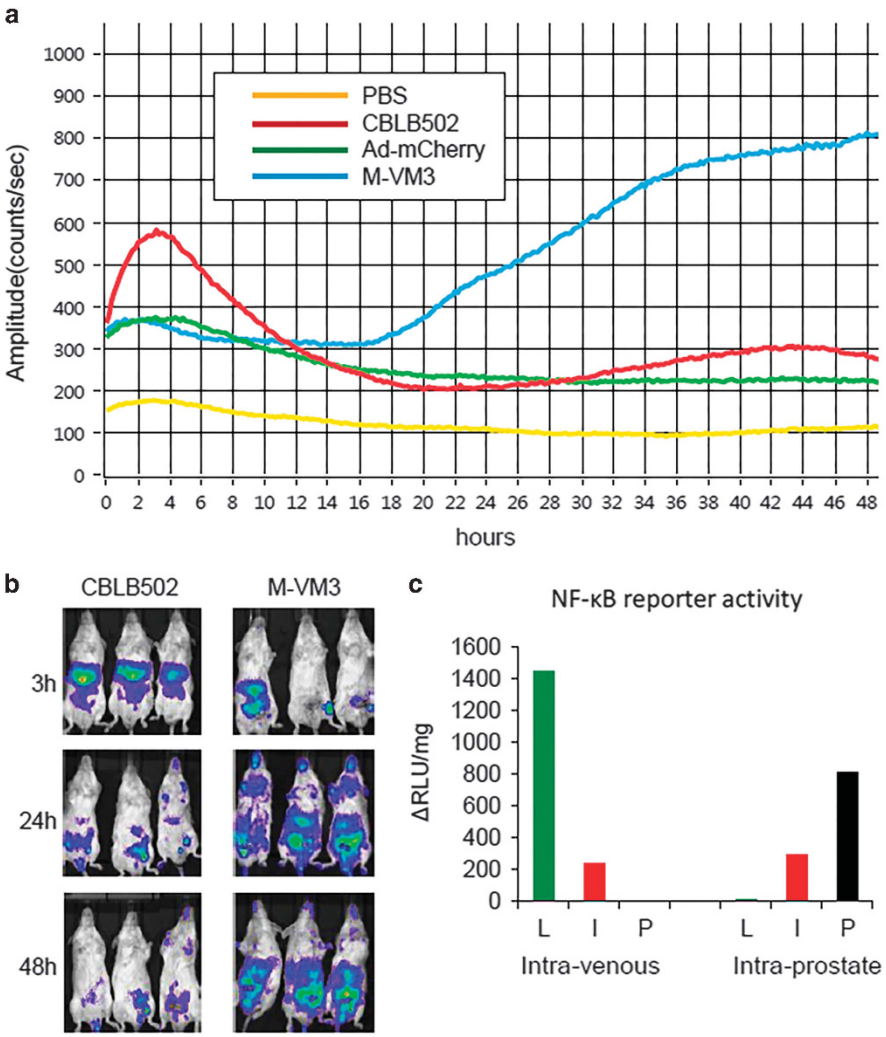

Figure 3. Induction of NF-κB activity in reporter mice after administration of M-VM3. (**a**) M-VM3 induces long-term activation of NF-κB in live mouse hepatocytes carrying an introduced NF-κB-dependent luciferase reporter construct. Cells were infected with M-VM3 (MOI = 10^4) or Ad-mCherry (MOI = 10^4) or treated with entolimod (0.1 mg/ml) or PBS (control), then these agents were removed from the media (3 h for Ad and 1 h for entolimod) and luciferase was measured by LumiCycle. The level of luciferase activity from PBS-treated cells was subtracted. (**b**) BALB/C-Tg(IkBa-luc)-Xen mice were given a single intraprostate injection of PBS, CBLB502 (1 μg per mouse) or M-VM3 (1×10^9 v.p.) and analyzed 3, 24 or 48 h later by whole-body Xenogen bio-luminescence imaging of live anesthetized animals. (**c**) Measurement of luciferase activity in liver (L), intestine (I) and prostate tissue (P) extracts of NF-κB-luciferase reporter mice BALB/C-Tg(IkBa-luc)-Xen after intravenous and intraprostate injections (48 h) of M-VM3. Relative light unit (RLU) values (per mg of total protein) in tissue extracts of M-VM3-treated mice were calculated by subtraction of RLU values for PBS-treated mice.

presence of prostate tumors and weight of each prostate lobe (anterior, dorsal, ventral and lateral) as a measure of tumor burden within the lobe. By this time, TRAMP males are known to develop epithelial hyperplasia in the prostate. In addition, hematoxylin and eosin-stained sections of prostate lobes were evaluated for morphological changes. The average weight of ventral lobes (the site of injection) was significantly lower in M-VM3-treated mice compared with Ad-mCherry and PBS controls (Figure 4a). The weight of other lobes was not significantly different between groups. These results provided an initial indication of M-VM3 antitumor efficacy in TRAMP mice.

Histological examination demonstrated that prostates from M-VM3-injected mice (Figure 4b), but not from those treated with PBS (Figure 4b) or Ad-mCherry (data not shown), contained single glands or groups of glands showing signs of atrophy and degeneration. This was particularly prominent in ventral lobes (site of injection) where glands appeared as an amorphous eosinophilic mass, with nuclei showing karyorhexis and karyolysis. In addition, increased presence of mononuclear (lymphoid/macrophage) cells was observed in the prostate interstitium of 12 of 15 M-VM3-treated mice (Figure 4b) but to a lesser degree in Ad-mCherry-treated animals (6 out of 15) and was not observed in PBS-treated mice (0 out of 14).

These findings suggest that M-VM3-induced accumulation of mononuclear/lymphoid cells in the prostate interstitium may be involved in antitumor immune responses capable of suppressing tumor growth and progression in the TRAMP model.

Intraprostate tumor injection of M-VM3 induces expression of genes involved in immune responses

To identify changes in gene expression underlying the observed mobilization of immune cells into prostate tumors following M-VM3 injection, we compared global gene expression profiles of TRAMP mouse prostate tumors 24 and 48 h after single i.t. injection of M-VM3, Ad-mCherry or vehicle using Illumina whole-genome microarrays (GEO repository, accession number GSE102023). At 24 h post-injection, 17 genes were induced more

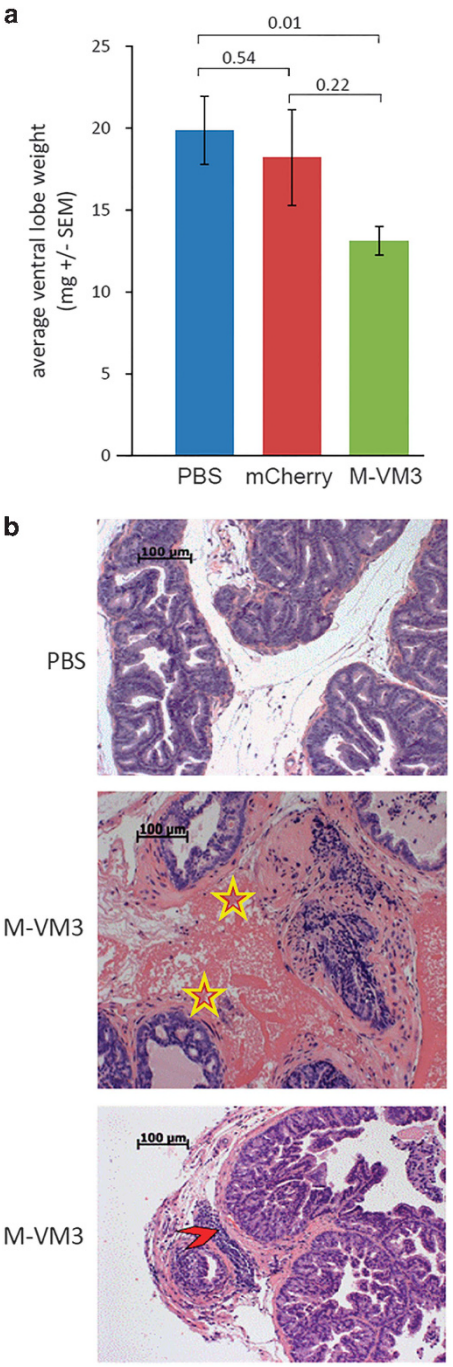

Figure 4. *In vivo* effect of M-VM3 on prostate tumors in mouse TRAMP model. (**a**) Average weight of prostate ventral lobes 6 weeks after intraprostate injections of M-VM3, Ad-mCherry and PBS of 45 12-week-old TRAMP mice (15 mice per group, error bars indicate s.e.m.). (**b**) Hematoxylin and eosin (H&E)-stained prostate sections were prepared 6 weeks after intraprostate injection of M-VM3 or PBS. Increased infiltration of lymphoid/mononuclear/macrophage cells (red arrowhead) in the interstitium between prostate lobes in M-VM3-injected TRAMP mice compared with PBS-injected TRAMP mice. Atrophic and degenerative changes (areas with yellow asterisks) in whole lobes of prostates from TRAMP mice treated with M-VM3.

strongly by M-VM3 than Ad-mCherry (Supplementary Table S1). Consistent with the known mechanisms of activation of TLR5 signaling by entolimod, this list includes several NF-κB target genes such as CXCL1, IL1B and S100A9. At 48 h, there was a larger number of genes specifically upregulated by M-VM3- versus Ad-mCherry (57 genes, Supplementary Table S2). This list includes a number of genes encoding cytokines/chemokines (IL1B, CCL7 and 9, CXCL9, 13 and 17), which may have roles in mobilization of immune cells into tumors. Other notable M-VM3-specific induced genes are several with known roles in regulation of NF-κB responses (for example, IKBKE and NFKBIZ) or antiviral activity (for example, NLRC5 and OASL1). Only four genes induced at 24 h remained induced at 48 h (NLRC5, CLEC4A1, IL1B and S100A9). In particular, M-VM3-induced NLRC5 may contribute to the anti-tumor immune response and prevention of tumor immune escape through activation of expression of MHC class-I molecules and components of the antigen-processing machinery.[45]

Intratumoral delivery of M-VM3 stimulates an innate immune response

To characterize immune cell infiltration into TRAMP prostate tumors in response to M-VM3, TRAMP mice with palpable prostate tumors were given an i.t. injection of PBS, Ad-mCherry or M-VM3 and prostate tumors and tumor-draining lymph nodes were collected 2 or 7 days later. As activation of TLR5 stimulates recruitment of neutrophils, NK cells and T cells to the liver,[6,8–10] we sought to characterize similar immune cell profiles in TRAMP prostate tumors by fluorescence-activated cell sorting analysis. Neutrophils were significantly recruited to the prostate on day 2 after i.t. delivery of M-VM3 or, to a lesser extent, after Ad-mCherry (Figure 5a). Although M-VM3 appeared to stimulate stronger recruitment of neutrophils than Ad-mCherry, this difference did not reach statistical significance. NK cells also responded to M-VM3, but not to Ad-mCherry and with kinetics that was different than for neutrophils and that was dependent upon virus identity (Figure 5b). M-VM3-specific induction of NK cells was not observed until day 7 post-i.t. injection.

We next characterized the response of adaptive immunity, which included $CD8^+$ and $CD4^+$ T cells. Levels of $CD8^+$ T cells in TRAMP tumors did not change following i.t. delivery of either Ad-mCherry or M-VM3 on day 7 (Figure 5c). Similar to the $CD8^+$ T-cell response, bona fide $CD4^+$ T cells, which we characterized as lacking FoxP3 expression and thus not Treg, showed no statistical difference at day 7 post-i.t. injection (Figure 5d). Finally, the effect of i.t. viral delivery on immunosuppressive Treg was characterized in TRAMP tumors and tumor-draining lymph node on day 7 post-i.t. injection. Levels of Tregs in TRAMP tumors (Figure 5e) and tumor-draining lymph nodes (Figure 5f) were not significantly affected by either virus.

Together, these data indicate that i.t. adenovirus (M-VM3 or Ad-mCherry) injection in TRAMP mice leads to recruitment of components of innate immunity to the prostate while having no impact on immunosuppressive Tregs. The main M-VM3-specific response was recruitment of NK cells to the prostate and, to a lesser extent, neutrophil recruitment.

Effect of M-VM3 on prostate tumor metastasis model

M-VM3 anti-metastatic activity was tested in a model in which metastatic outgrowth of TRAMP-C2 prostate cancer occurs after primary tumor resection.[46] Mice with s.c. growing TRAMP-C2 tumors (~100 mm^3) were given a single i.t. injection of PBS, Ad-mCherry or M-VM3. Primary tumors were removed 7 days post-injection and the animals were monitored for survival until day 150 post-injection. As shown in Figure 6a, M-VM3 injection before tumor removal improved survival to day 150 compared with PBS and Ad-mCherry. Log-rank analysis showed that the difference in mortality kinetics between the M-VM3-treated and control groups was nearly statistically significant ($P = 0.06$). These results indicate that M-VM3 has a potential to be effective in combination with surgery to prevent prostate tumor metastasis.

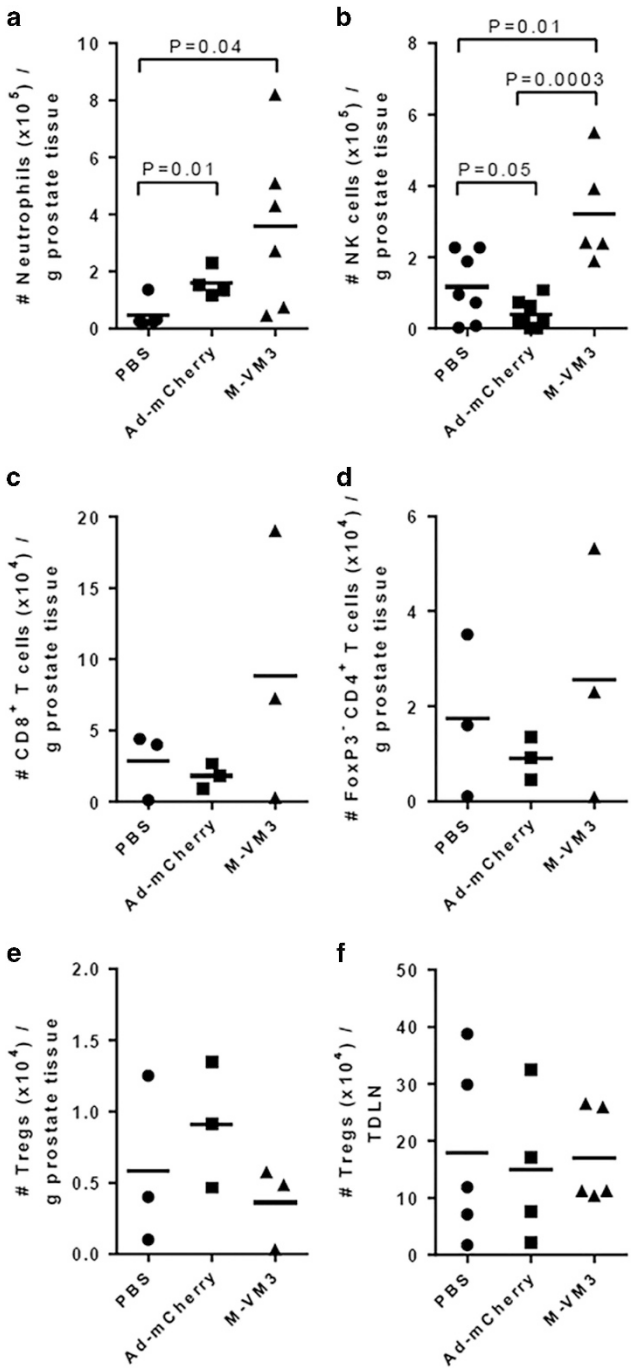

Figure 5. Quantitative analysis of innate and adaptive immune cell populations recruited to TRAMP tumors and tumor-draining lymph nodes (TDLNs) following i.t. injection of Ad-mCherry or M-VM3. Palpable spontaneously developed prostate tumors (**a**–**e**) and TDLNs (**f**) from tumor-bearing TRAMP mice were collected 2 (for neutrophils) or 7 days (for NK and T cells) after i.t. injection of PBS (vehicle), Ad-mCherry (control) or M-VM3 (10^9 v.p total per three points). Specific immune cell populations within the samples were quantified by fluorescence-activated cell sorting (FACS) and are reported as absolute number of cells per gram of prostate tissue or per TDLN. (**a**) Neutrophils were defined as $CD45^+CD11b^+CD11c^-Ly\text{-}6C^{lo/-}Ly\text{-}6G^{hi}$; (**b**) NK cells were defined as $CD45^+CD3\varepsilon^-NK1.1^+$; (**c**) $CD8^+$ T cells were defined as $CD45^+CD3\varepsilon^+CD8^+$; (**d**) $CD4^+$ T cells were defined as $CD45^+CD3\varepsilon^+FoxP3^-CD4^+$; and (**e, f**) Tregs were defined as $CD45^+CD3\varepsilon^+CD4^+FoxP3^+$ in tumors and TDLN. Data are shown as mean ± s.e.m. ($N = 3$–7 mice per group).

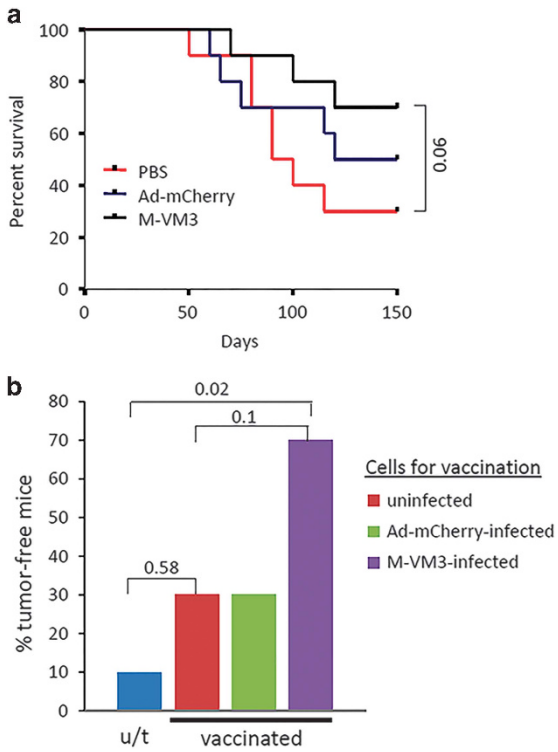

Figure 6. Antitumor effects of M-VM3. (**a**) TRAMP-C2 tumors were grown s.c. in C57BL/6 mice and injected i.t. with PBS, Ad-mCherry (5×10^8 v.p.) or M-VM3 (5×10^8 v.p.) on day 0. Tumors were surgically removed on day 7 and the mice were monitored for survival in a blinded manner until day 150. (**b**) C57BL/6 mice ($n = 10$ per group) were vaccinated s.c. with M-VM3- or Ad-mCherry-infected (irradiated 48 h after virus infection) or uninfected irradiated TRAMP-C2 cells. A fourth group of mice was not vaccinated. Mice were vaccinated on days 0, 14 and 21 and then challenged with TRAMP-C2 cells by s.c. injection 14 days after the last vaccination. Tumor growth was monitored for 38 days post-challenge or until tumors reached the endpoint size that required killing. Percentage of tumor-free mice was determined at day 38 post-challenge.

Antitumor vaccination by M-VM3-transduced tumor cells

Stimulation of antitumor immunity by M-VM3 suggested that it may be useful not only as a therapy, but also as a prophylactic anticancer vaccine. To test this possibility, TRAMP-C2 cells were infected with M-VM3, lethally irradiated 48 h later, and then used to vaccinate C57BL/6 mice. Control groups were not vaccinated or vaccinated with similarly prepared Ad-mCherry-infected or -uninfected cells. Mice were vaccinated s.c. on study days 0, 14 and 21 and challenged with TRAMP-C2 cells by s.c. injection 14 days after the last vaccination. S.c. tumor growth was monitored for 38 days post-challenge or until tumors reached the endpoint size that required killing. The percentage of mice that developed tumors was significantly lower in the group immunized with M-VM3-infected cells compared with all three control groups (Figure 6b) thus indicating efficacy of the tested M-VM3-based vaccination strategy.

DISCUSSION

Immunotherapeutic strategies aimed at stimulating the immune system to attack cancer cells or blocking immunosuppressive mechanisms hold strong promise for improving cancer treatment. Our work and that of others has identified TLR5 activation as a particularly attractive means to stimulate antitumor immune responses (reviewed in Introduction).[2–11] To expand clinical

applications of TLR5-mediated immunotherapy to include tumors that do not naturally express TLR5, we generated a novel adenoviral vector, Mobilan-VM3, which directs co-expression of TLR5 and a secreted entolimod-based TLR5 agonist and thereby expected to establish intrinsic TLR5 activation in transduced tumor cells localized and restricted to the injection site.

The ability of Mobilan to overcome the natural mechanisms that shut down TLR5 signaling consequently limit the immunostimulatory ability of extrinsically applied TLR5 agonists, like entolimod, was demonstrated using an NF-κB reporter system in cell culture and *in vivo*. In both cases, Mobilan was capable of maintaining greater constitutive and higher NF-κB signaling than entolimod. One more important advantage of Mobilan is the resistance of its activity as a TLR5 activator to neutralizing antibodies, which completely abolish the activity of entolimod, and prevent a significant proportion of the human population from the benefits offered by treatment with this agent.

Prostate cancer models were used for *in vivo* testing as a prospective clinical target disease for Mobilan. This choice has been made based on several considerations. First, a high frequency of CAR expression in normal and cancerous prostate epithelium shown in the present work is consistent with previous demonstration of efficient infection of prostate tumors by adenoviruses;[47] we confirmed efficient transduction of mouse prostate tumors (*in vivo*) and surgical specimens of human prostate tumors (*ex vivo)* upon direct i.t. injection of our adenoviral vectors. Second, the prostate is relatively easily accessible for intra-organ injection with Mobilan, allowing us to develop a clinically translatable treatment protocol. Third, prostate does not belong to the group of organs with high expression of TLR5; therefore, Mobilan has the opportunity to induce TLR5 signaling in TLR5-negative organs, which are not among the targets of entolimod. Also, the efficacy of type 5 adenovirus infection of cells depends on the level of CAR receptor expression on their surface. Cells of hematopoietic origin that do not express CAR cannot be transduced with vectors based on a type 5 adenovirus.[48]

One of the biggest concerns about systemic use of TLR agonists is their safety. Acute systemic inflammatory response induced following systemic administration of TLR agonists has prevented development of a variety of TLR agonists into approved drugs.[49] And the only one currently approved by the FDA, imiquimod, is allowed exclusively for topical applications.[50] We hoped that the level of TLR5 agonist expression by Mobilan-VM3 would prevent this safety concern by producing a sufficient amount of agonist for intrinsic TLR5 signaling activation but not enough for systemic effects. In fact, unlike entolimod treatment, M-VM3 established continuous local (but not systemic) TLR5 signaling in TRAMP prostate cancer cells and in mouse prostate tissue following intraprostate injection. These results highlight another important advantage of Mobilan—its localized activity restricted to the injection site.

Efficacy of TLR5 agonists as antitumor immunotherapeutic agents has been demonstrated in multiple preclinical models. The antitumor activity of flagellin in mice bearing breast cancer xenografts was associated with increased tumor necrosis and enhanced infiltration of neutrophils into tumors.[6] Entolimod-driven recruitment of NK cells to the liver was shown to be critical for the antitumor efficacy of the drug in murine tumor models.[8,10] It was previously shown in TLR5-positive human prostate cancer cell lines LNCaP and DU-145 that flagellin induces chemokines that recruit NK cells and cytotoxic $CD8^+$ T cells, which may contribute to tumor inhibition.[51] Leigh *et al*.[52] demonstrated that activity of entolimod against lymphoma involved NK and $CD8^+$ T cells. In murine colon and mammary metastatic cancer models, entolimod supported homing of NK cells to the liver followed by NK cell-dependent activation of dendritic cells and antitumor $CD8^+$ T-cell responses.[9] We expected Mobilan to utilize all these antitumor mechanisms in a localized organ-specific setting. In fact, injection of M-VM3 into TRAMP prostate tumors suppressed tumor progression (indicated by tumor weight and histology) and led to recruitment of innate immunity, including neutrophils and NK cells. Involvement of these immune mechanisms can be explained by the profile of M-VM3-specific gene expression observed in our microarray experiments and is consistent with earlier studies with flagellin and entolimod. Remarkably, indications of antitumor efficacy of M-MV3 in the TRAMP model was demonstrated even with no detectable increase in T cells, suggesting that the therapeutic effect is driven predominantly by an innate immune response. It remains unclear whether lack of T-cell engagement is a property of the model or the prostate as an organ.

Potential use of TLR5 agonists to stimulate antitumor immune responses is supported by studies evaluating flagellin as a vaccine adjuvant. Co-administration of flagellin with MHC class II-restricted P10[53] or E6/E7 peptides[54] or with an adenovirus expressing the MUC-1 tumor antigen[55] led to improved antitumor effects of the vaccines. Beneficial effects of flagellin were also observed in the contexts of an adenovirus expressing a chaperone Grp170-flagellin chimera,[56] liposomes engrafted with flagellin-derived peptides and containing the model antigen ovalbumin,[57] and tumor cells[2,21] and T cells[58] engineered to express flagellin. In our study, a single i.t. injection of M-VM3 into s.c. growing TRAMP-C2 tumors improved mouse survival after surgical removal of the tumors, suggesting that i.t. vaccination with M-VM3 may be an effective strategy for preventing metastasis in prostate cancer patients. We also found that vaccination of mice with lethally irradiated M-VM3-infected TRAMP-C2 cells (prime + 2 boosts) protected mice against a subsequent s.c. challenge with TRAMP-C2 cells. Use of cell-based vaccination against prostate cancer is illustrated by Sipuleucel-T, an FDA-approved autologous cellular vaccine consisting of a patient's dendritic cells loaded with a prostatic acid phosphatase-granulocyte/macrophage colony-stimulating factor fusion protein.[21] Sipuleucel-T prolonged survival in men with metastatic prostate cancer but had no effect on time to progression.[59] Trials with GVAX, a vaccine comprised of prostate cancer cell lines (LNCaP and PC3) expressing GM-CSF were terminated because of a lack of overall survival benefit.[21–24] Our data suggest that M-VM3 could fill the need for more effective cell-based vaccines against prostate cancer. The first step in this direction is an ongoing Phase I clinical trial, in which M-VM3 is used for intraprostate injection 2 weeks before radical prostatectomy (ClinicalTrials.gov Identifier: NCT02654938). Future work will address the possibility of achieving greater antitumor effects by combining M-VM3 with immune checkpoint inhibitors (CTLA-4, PD1/PD-L1) that have shown activity against different tumors.[29–36]

Overall, this work provides proof-of-concept for use of M-VM3 to establish constitutive TLR5 signaling in tumors regardless of their TLR5 expression status and demonstrates that such signaling leads to antitumor immune responses capable of suppressing prostate tumor development, progression and metastasis in different experimental settings.

MATERIALS AND METHODS

Mice

C57BL/6 mice (6- to 8-week-old males) were obtained from Taconic, Inc. (Hudson, NY, USA). TRAMP mice[37] were bred in the RPCI (Mouse Tumor Model Resource). BALB/C-Tg(IκBα-luc)-Xen mice (carrying an IKBα promoter-controlled firefly luciferase reporter transgene) were purchased from Xenogen Corporation (Alameda, CA, USA) and maintained as a colony in the RPCI animal facility. TLR5KO mice (B6.129S1-*Tlr5*^{tm1Flv}/J) were purchased from The Jackson Laboratories (Bar Harbor, ME, USA) and maintained as above. All animal studies were conducted in accordance with the recommendations in the Guide for the Care and Use of Laboratory Animals of the Association for the Assessment and Accreditation of Laboratory Animal Care International (AAALAC). The experiment protocol was approved by the Institutional Animal Care and Use Committee (IACUC) at the Roswell Park Cancer Institute (protocol # 1081). Animals were

assigned randomly to groups; group sizes were selected based on prior experience. No animals were excluded from further analyses in the reported studies.

Reagents

Rabbit anti-CBLB502 polyclonal antibody (pAb), biotin-labeled goat anti-CBLB502 pAb and 1B04 anti-human TLR5 monoclonal antibody (mAb) were produced by Cleveland BioLabs, Inc. (CBLI; Buffalo, NY, USA). Antibodies for immunohistology included rabbit polyclonal anti-NF-κB p65 (catalog #7970; Abcam, Cambridge, UK), rat monoclonal anti-cytokeratin 8 (Troma-1; Developmental Studies Hybridoma Bank, University of Iowa, Iowa City, IA, USA) and anti-CAR antibody (H-300; catalog #sc-15405, Santa Cruz, CA, USA). Tumor necrosis factor-α was purchased from PeproTech Inc. (Rocky Hill, NJ, USA), and lipopolysaccharide from *E. coli* 055:B5 was purchased from Sigma-Aldrich (St Louis, MO, USA). CBLB502 and CBLB502NQ were produced as described.[60]

Cultured cells

The TRAMP-C2 prostate cancer cells maintained as described.[37] To develop stable NF-κB-luc reporter cell lines, MOSEC cells (from Dr A Odunsi, RPCI, Buffalo, NY, USA) and TRAMP-C2 cells were transduced with Lenti NF-κB Reporter (QIAGEN, Frederick, MD, USA) followed by puromycin selection. Primary mouse hepatocytes were isolated as described.[61] All cell lines were tested for mycoplasma contamination (MycoAlert Mycoplasma Detection assay, Lonza, Rockland, ME, USA). No authentication of the cell lines was conducted by the authors.

Adenoviruses

Adenovirus constructs (Ad-mCherry, Mobilan M-0 and M-VM3) were prepared using the AdMax system (Microbix Biosystems, Mississauga, Canada). Expression cassettes were assembled in shuttle plasmid pDC515 and Ad genomic plasmid pBHGloxΔE1,3 Cre was used for recombination to obtain final constructs. Resulting viruses were plaque-purified, amplified and purified in CsCl gradient. Mobilan M-0, M-VM3 and Ad-mCherry stocks contained 1×10^{12}, 1.1×10^{12} and 1×10^{12} vp/ml, respectively.

Luciferase assays

NF-κB-dependent luciferase expression in reporter cell lines and in extracts of reporter mouse organs was measured as described in references Yoon *et al*.[60] and Burdelya *et al*.,[44] respectively.

Imaging of NF-κB-driven luciferase expression in live mice

Three-month-old males of Balb/C-Tg(IκBα-luc)Xen NF-κB reporter mice were used. Bio-luminescence imaging was performed using the IVIS50 imaging system (PerkinElmer, Waltham, MA, USA) as described.[44]

NF-κB-driven luciferase expression in live cells

Mouse NF-κB-luc-hepatocytes were infected with M-VM3 or Ad-mCherry (multiplicity of infection (MOI) = 10^4) or treated with entolimod (0.1 μg/ml) or PBS. The virus-containing medium was replaced with fresh medium after 3 h (1 h in case of entolimod) and luciferin was added to the cells. Luciferase activity was measured in LumiCycle 32 (Actimetrics, Wilmette, IL, USA) for 3 days. Baseline level of luciferase activity was subtracted.

ELISA and western blot

CBLB502 and its derivatives were detected by ELISA[62] and western blot using CBLB502-specific pAbs and TLR5 was detected by western blot using 1B04 mAb (see Reagents).

Histochemistry and immunohistochemistry

Sections of tumor tissues and cultured cells were stained as described.[44] Primary antibodies: anti-NF-κB p65 (Abcam, cat. #7970), anti-cytokeratin 8 (Troma-1; Developmental Studies Hybridoma Bank, University of Iowa), anti-CAR (Santa Cruz, cat.#sc-15405) and anti-integrin alpha 6 (Abcam, cat. #ab62844-100). Images were obtained using an Axio Imager Z1 (Carl Zeiss, Jena, Germany) fluorescent microscope equipped with a high sensitivity CCD digital camera MRm (Carl Zeiss, Jena, Germany) and AxioVision software (release 4.8.3) (Carl Zeiss, Jena, Germany). Individual, manual scoring of tissue microarray samples was performed using the ImageScope image viewer from Aperio (Aperio Technologies, Vista, CA, USA). Intensity was recorded/scored in a semiquantitative manner.[63] Evaluation of blinded histological sections was performed by trained pathologist.

Deglycosylation of CBLB502

MOSEC cultures at 50% confluence were infected with M-0 (1×10^9 v.p./ml). After 48 h, cell extracts were prepared using CelLytic M (Sigma-Aldrich). Lysates were cleared by centrifugation and desalted using spin columns. Deglycosylation was performed with the Protein Deglycosylation Mix reagent kit (New England Biolabs, Ipswich, MA, USA) according to the manufacturer's protocol.

Infection of mouse and human tumors with Ad-mCherry

In total, 1×10^7 TRAMP-C2 cells were injected into mice s.c. Ad-mCherry (2×10^9 v.p.in total) was injected in three different points of each tumor (~100 mm^3). Samples of human prostate tumors (received from RPCI; non-human subject research, Protocol NHR028412 approved by DSRG/Tissue Group) were dissected into $0.5\times0.5\times1$ cm pieces and two pieces from each patient were injected with Ad-mCherry as for mouse tumors. Injected human samples were cultured in enriched Dulbecco's modified Eagle's medium additionally supplemented with 5 μg/ml insulin and 10^{-8} M dihydrotestosterone at 37 °C, 5% CO_2.

Prostate injection

The abdomens of anesthetized TRAMP mice were shaved. Using aseptic technique, a 1 cm incision was made with scissors above the prostate on the ventral side of the animal through the skin and body wall and 10^9 v.p. (50 μl in total) of M-VM3, Ad-mCherry or PBS were injected into three points of the prostate ventral lobe. The body wall was closed with 1–2 sutures and the skin was closed with wound clips.

Cell-based immunization of mice

In all, 70% confluent TRAMP-C2 cells were infected with M-VM3 or Ad-mCherry (MOI = 1.2×10^5) and 48 h later irradiated (50 Gy dose, Gamma irradiator Shepherd 4 000 Ci Cesium-137 source). C57BL/6 mice ($n=10$ per group) were left unvaccinated or vaccinated s.c. with uninfected, M-VM3- or Ad-mCherry-infected cells (1×10^6 cells per mouse) on study days 0, 14 and 21. Mice were challenged with TRAMP-C2 cells (1×10^7 cells per mouse, s.c. injection) 14 days after the last vaccination. Tumor growth was monitored for 38 days post-challenge.

Surgical removal of TRAMP-C2 tumors after i.t. injection M-VM3

Tumors (~100 mm^3) that developed in C57BL/6 mice 4 weeks after TRAMP-C2 cell s.c. inoculation (1×10^7 cells per mouse) were injected i.t. with PBS, Ad-mCherry (10^8 vp) or M-VM3 (10^8 vp) (50 μl/tumor). Tumors were surgically removed 7 days post-injection as described.[46]

Fluorescence-activated cell sorting analysis of immune cell populations

M-VM3- or Ad-mCherry- or PBS-injected tumors were harvested 2, 7 or 14 days post-injection and weighed. Single-cell suspensions were generated and analyzed by fluorescence-activated cell sorting as described.[44]

Microarray analysis

Gene expression profiling was accomplished by the RPCI Genomics Shared Facility using Mouse WG-6 whole-genome gene expression assay and direct hybridization assay (Illumina, San Diego, CA, USA). RNA was prepared 24 and 48 h after injection with M-VM3, Ad-mCherry (10^9 v.p, 50 μl total into three points) or PBS (two mice per group) into palpable spontaneous prostate tumors of TRAMP mice (22–26 weeks old). Quantile normalization and background subtraction was conducted using Illumina Genestudio. Genes that had a minimum signal of 50 in both adenoviral-infected replicates and were induced at least twofold by Ad-mCherry or M-VM3 as compared with PBS were considered induced for the purposes of analysis.

Statistical analysis

One representative experimental data set is shown from two or three independent experiments. Differences between groups within experiments were analyzed using two-tailed unpaired Student's *t*-test and Fisher's exact test. Animal survival Kaplan–Meier curves were compared using log-rank test. $P < 0.05$ was considered statistically significant.

CONFLICT OF INTEREST

The authors declare no conflict of interest.

ACKNOWLEDGEMENTS

We thank Cellecta, Inc. and O.D.260, Inc. help with for adenoviral vector construction and manufacturing. This work was supported by contract from Panacela Labs (a biotech company that possesses intellectual property rights for Mobilan), LLC, National Cancer Institute (NCI) Cancer Center Core Grant P30CA016056 and by grants from DOD (BC140507 to AVG) the Roswell Park Alliance Foundation to EAK and AVG.

AUTHOR CONTRIBUTIONS

VM, EAK and AVG designed the study and interpreted the data. KG, IB, BG, CB, ASG, IAT, SA-S, EK, MB-N, OVK and ALO conducted experiments. CJ, CM, MTM and BAF provided critically important models and research tool and participated in data interpretation. VM, EAK, PSB and AVG wrote the manuscript.

REFERENCES

1 Eaves-Pyles TD, Wong HR, Odoms K, Pyles RB. Salmonella flagellin-dependent proinflammatory responses are localized to the conserved amino and carboxyl regions of the protein. *J Immunol* 2001; **167**: 7009–7016.
2 Garaude J, Kent A, van Rooijen N, Blander JM. Simultaneous targeting of toll- and nod-like receptors induces effective tumor-specific immune responses. *Sci Transl Med* 2012; **4**: 120ra116.
3 Rhee SH, Im E, Pothoulakis C. Toll-like receptor 5 engagement modulates tumor development and growth in a mouse xenograft model of human colon cancer. *Gastroenterology* 2008; **135**: 518–528.
4 Sfondrini L, Rossini A, Besusso D, Merlo A, Tagliabue E, Menard S *et al.* Antitumor activity of the TLR-5 ligand flagellin in mouse models of cancer. *J Immunol* 2006; **176**: 6624–6630.
5 Soto LJ 3rd, Sorenson BS, Kim AS, Feltis BA, Leonard AS, Saltzman DA. Attenuated Salmonella typhimurium prevents the establishment of unresectable hepatic metastases and improves survival in a murine model. *J Pediatr Surg* 2003; **38**: 1075–1079.
6 Cai Z, Sanchez A, Shi Z, Zhang T, Liu M, Zhang D. Activation of Toll-like receptor 5 on breast cancer cells by flagellin suppresses cell proliferation and tumor growth. *Cancer Res* 2011; **71**: 2466–2475.
7 Burdelya LG, Gleiberman AS, Toshkov I, Aygun-Sunar S, Bapardekar M, Manderscheid-Kern P *et al.* Toll-like receptor 5 agonist protects mice from dermatitis and oral mucositis caused by local radiation: implications for head-and-neck cancer radiotherapy. *Int J Radiat Oncol Biol Phys* 2012; **83**: 228–234.
8 Burdelya LG, Brackett CM, Kojouharov B, Gitlin II, Leonova KI, Gleiberman AS *et al.* Central role of liver in anticancer and radioprotective activities of Toll-like receptor 5 agonist. *Proc Natl Acad Sci USA* 2013; **110**: E1857–E1866.
9 Brackett CM, Kojouharov B, Veith J, Greene KF, Burdelya LG, Gollnick SO *et al.* Toll-like receptor-5 agonist, entolimod, suppresses metastasis and induces immunity by stimulating an NK-dendritic-CD8+ T-cell axis. *Proc Natl Acad Sci USA* 2016; **113**: E874–E883.
10 Yang H, Brackett CM, Morales-Tirado VM, Li Z, Zhang Q, Wilson MW *et al.* The Toll-like receptor 5 agonist entolimod suppresses hepatic metastases in a murine model of ocular melanoma via an NK cell-dependent mechanism. *Oncotarget* 2016; **7**: 2936–2950.
11 Yam C, Zhao M, Hayashi K, Ma H, Kishimoto H, McElroy M *et al.* Monotherapy with a tumor-targeting mutant of S. typhimurium inhibits liver metastasis in a mouse model of pancreatic cancer. *J Surg Res* 2010; **164**: 248–255.
12 Mizel SB, Bates JT. Flagellin as an adjuvant: cellular mechanisms and potential. *J Immunol* 2010; **185**: 5677–5682.
13 Rhee SH. Basic and translational understandings of microbial recognition by toll-like receptors in the intestine. *J Neurogastroenterol Motil* 2011; **17**: 28–34.
14 Cuadros C, Lopez-Hernandez FJ, Dominguez AL, McClelland M, Lustgarten J. Flagellin fusion proteins as adjuvants or vaccines induce specific immune responses. *Infect Immun* 2004; **72**: 2810–2816.
15 Means TK, Hayashi F, Smith KD, Aderem A, Luster AD. The Toll-like receptor 5 stimulus bacterial flagellin induces maturation and chemokine production in human dendritic cells. *J Immunol* 2003; **170**: 5165–5175.
16 Kaczanowska S, Joseph AM, Davila E. TLR agonists: our best frenemy in cancer immunotherapy. *J Leukocyte Biol* 2013; **93**: 847–863.
17 Akira S, Takeda K. Functions of toll-like receptors: lessons from KO mice. *C R Biol* 2004; **327**: 581–589.
18 Carvalho FA, Aitken JD, Gewirtz AT, Vijay-Kumar M. TLR5 activation induces secretory interleukin-1 receptor antagonist (sIL-1Ra) and reduces inflammasome-associated tissue damage. *Mucosal Immunol* 2011; **4**: 102–111.
19 Vijay-Kumar M, Carvalho FA, Aitken JD, Fifadara NH, Gewirtz AT. TLR5 or NLRC4 is necessary and sufficient for promotion of humoral immunity by flagellin. *Eur J Immunol* 2010; **40**: 3528–3534.
20 Hemmi S, Geertsen R, Mezzacasa A, Peter I, Dummer R. The presence of human coxsackievirus and adenovirus receptor is associated with efficient adenovirus-mediated transgene expression in human melanoma cell cultures. *Hum Gene Ther* 1998; **9**: 2363–2373.
21 Fernandez-Garcia EM, Vera-Badillo FE, Perez-Valderrama B, Matos-Pita AS, Duran I. Immunotherapy in prostate cancer: review of the current evidence. *Clin Transl Oncol* 2015; **17**: 339–357.
22 Shi Y, Liu CH, Roberts AI, Das J, Xu G, Ren G *et al.* Granulocyte-macrophage colony-stimulating factor (GM-CSF) and T-cell responses: what we do and don't know. *Cell Res* 2006; **16**: 126–133.
23 Dranoff G, Jaffee E, Lazenby A, Golumbek P, Levitsky H, Brose K *et al.* Vaccination with irradiated tumor cells engineered to secrete murine granulocyte-macrophage colony-stimulating factor stimulates potent, specific, and long-lasting anti-tumor immunity. *Proc Natl Acad Sci USA* 1993; **90**: 3539–3543.
24 Simons JW, Sacks N. Granulocyte-macrophage colony-stimulating factor-transduced allogeneic cancer cellular immunotherapy: the GVAX vaccine for prostate cancer. *Urol Oncol* 2006; **24**: 419–424.
25 Michael A, Ball G, Quatan N, Wushishi F, Russell N, Whelan J *et al.* Delayed disease progression after allogeneic cell vaccination in hormone-resistant prostate cancer and correlation with immunologic variables. *Clin Cancer Res* 2005; **11**: 4469–4478.
26 Korman AJ, Peggs KS, Allison JP. Checkpoint blockade in cancer immunotherapy. *Adv Immunol* 2006; **90**: 297–339.
27 Arlen PM, Skarupa L, Pazdur M, Seetharam M, Tsang KY, Grosenbach DW *et al.* Clinical safety of a viral vector based prostate cancer vaccine strategy. *J Urol* 2007; **178**: 1515–1520.
28 Lubaroff DM, Konety BR, Link B, Gerstbrein J, Madsen T, Shannon M *et al.* Phase I clinical trial of an adenovirus/prostate-specific antigen vaccine for prostate cancer: safety and immunologic results. *Clin Cancer Res* 2009; **15**: 7375–7380.
29 Kwon ED, Drake CG, Scher HI, Fizazi K, Bossi A, van den Eertwegh AJ *et al.* Ipilimumab versus placebo after radiotherapy in patients with metastatic castration-resistant prostate cancer that had progressed after docetaxel chemotherapy (CA184-043): a multicentre, randomised, double-blind, phase 3 trial. *Lancet Oncol* 2014; **15**: 700–712.
30 Topalian SL, Hodi FS, Brahmer JR, Gettinger SN, Smith DC, McDermott DF *et al.* Safety, activity, and immune correlates of anti-PD-1 antibody in cancer. *N Engl J Med* 2012; **366**: 2443–2454.
31 Sullivan RJ, Lorusso PM, Flaherty KT. The intersection of immune-directed and molecularly targeted therapy in advanced melanoma: where we have been, are, and will be. *Clin Cancer Res* 2013; **19**: 5283–5291.
32 Ott PA, Hodi FS, Robert C. CTLA-4 and PD-1/PD-L1 blockade: new immunotherapeutic modalities with durable clinical benefit in melanoma patients. *Clin Cancer Res* 2013; **19**: 5300–5309.
33 Mamalis A, Garcha M, Jagdeo J. Targeting the PD-1 pathway: a promising future for the treatment of melanoma. *Arch Dermatol Res* 2014; **306**: 511–519.
34 Forde PM, Reiss KA, Zeidan AM, Brahmer JR. What lies within: novel strategies in immunotherapy for non-small cell lung cancer. *Oncologist* 2013; **18**: 1203–1213.
35 Pardoll DM. The blockade of immune checkpoints in cancer immunotherapy. *Nat Rev Cancer* 2012; **12**: 252–264.
36 Brahmer JR, Tykodi SS, Chow LQ, Hwu WJ, Topalian SL, Hwu P *et al.* Safety and activity of anti-PD-L1 antibody in patients with advanced cancer. *N Engl J Med* 2012; **366**: 2455–2465.
37 Foster BA, Gingrich JR, Kwon ED, Madias C, Greenberg NM. Characterization of prostatic epithelial cell lines derived from transgenic adenocarcinoma of the mouse prostate (TRAMP) model. *Cancer Res* 1997; **57**: 3325–3330.
38 Greenberg NM, DeMayo F, Finegold MJ, Medina D, Tilley WD, Aspinall JO *et al.* Prostate cancer in a transgenic mouse. *Proc Natl Acad Sci USA* 1995; **92**: 3439–3443.

39 Gingrich JR, Greenberg NM. A transgenic mouse prostate cancer model. *Toxicol Pathol* 1996; **24**: 502–504.
40 Gupta S, Ahmad N, Marengo SR, MacLennan GT, Greenberg NM, Mukhtar H. Chemoprevention of prostate carcinogenesis by alpha-difluoromethylornithine in TRAMP mice. *Cancer Res* 2000; **60**: 5125–5133.
41 Hurwitz AA, Foster BA, Kwon ED, Truong T, Choi EM, Greenberg NM *et al.* Combination immunotherapy of primary prostate cancer in a transgenic mouse model using CTLA-4 blockade. *Cancer Res* 2000; **60**: 2444–2448.
42 Mentor-Marcel R, Lamartiniere CA, Eltoum IE, Greenberg NM, Elgavish A. Genistein in the diet reduces the incidence of poorly differentiated prostatic adenocarcinoma in transgenic mice (TRAMP). *Cancer Res* 2001; **61**: 6777–6782.
43 Kaplan-Lefko PJ, Chen TM, Ittmann MM, Barrios RJ, Ayala GE, Huss WJ *et al.* Pathobiology of autochthonous prostate cancer in a pre-clinical transgenic mouse model. *Prostate* 2003; **55**: 219–237.
44 Burdelya LG, Krivokrysenko VI, Tallant TC, Strom E, Gleiberman AS, Gupta D *et al.* An agonist of toll-like receptor 5 has radioprotective activity in mouse and primate models. *Science* 2008; **320**: 226–230.
45 Rodriguez GM, Bobbala D, Serrano D, Mayhue M, Champagne A, Saucier C *et al.* NLRC5 elicits antitumor immunity by enhancing processing and presentation of tumor antigens to CD8(+) T lymphocytes. *Oncoimmunology* 2016; **5**: e1151593.
46 Kwon ED, Foster BA, Hurwitz AA, Madias C, Allison JP, Greenberg NM *et al.* Elimination of residual metastatic prostate cancer after surgery and adjunctive cytotoxic T lymphocyte-associated antigen 4 (CTLA-4) blockade immunotherapy. *Proc Natl Acad Sci USA* 1999; **96**: 15074–15079.
47 Rauen KA, Sudilovsky D, Le JL, Chew KL, Hann B, Weinberg V *et al.* Expression of the coxsackie adenovirus receptor in normal prostate and in primary and metastatic prostate carcinoma: potential relevance to gene therapy. *Cancer Res* 2002; **62**: 3812–3818.
48 Marini FC 3rd, Yu Q, Wickham T, Kovesdi I, Andreeff M. Adenovirus as a gene therapy vector for hematopoietic cells. *Cancer Gene Ther* 2000; **7**: 816–825.
49 Glavan TM, Pavelic J. The exploitation of Toll-like receptor 3 signaling in cancer therapy. *Curr Pharma Design* 2014; **20**: 6555–6564.
50 Meyer T, Stockfleth E. Clinical investigations of Toll-like receptor agonists. *Exp Opin Investig Drugs* 2008; **17**: 1051–1065.
51 Galli R, Starace D, Busa R, Angelini DF, Paone A, De Cesaris P *et al.* TLR stimulation of prostate tumor cells induces chemokine-mediated recruitment of specific immune cell types. *J Immunol* 2010; **184**: 6658–6669.
52 Leigh ND, Bian G, Ding X, Liu H, Aygun-Sunar S, Burdelya LG *et al.* A flagellin-derived toll-like receptor 5 agonist stimulates cytotoxic lymphocyte-mediated tumor immunity. *PLoS ONE* 2014; **9**: e85587.
53 de Melo FM, Braga CJ, Pereira FV, Maricato JT, Origassa CS, Souza MF *et al.* Anti-metastatic immunotherapy based on mucosal administration of flagellin and immunomodulatory P10. *Immunol Cell Biol* 2015; **93**: 86–98.
54 Lee SE, Hong SH, Verma V, Lee YS, Duong TN, Jeong K *et al.* Flagellin is a strong vaginal adjuvant of a therapeutic vaccine for genital cancer. *Oncoimmunology* 2016; **5**: e1081328.
55 Tosch C, Geist M, Ledoux C, Ziller-Remi C, Paul S, Erbs P *et al.* Adenovirus-mediated gene transfer of pathogen-associated molecular patterns for cancer immunotherapy. *Cancer Gene Ther* 2009; **16**: 310–319.
56 Yu X, Guo C, Yi H, Qian J, Fisher PB, Subjeck JR *et al.* A multifunctional chimeric chaperone serves as a novel immune modulator inducing therapeutic antitumor immunity. *Cancer Res* 2013; **73**: 2093–2103.
57 Faham A, Altin JG. Antigen-containing liposomes engrafted with flagellin-related peptides are effective vaccines that can induce potent antitumor immunity and immunotherapeutic effect. *J Immunol* 2010; **185**: 1744–1754.
58 Kaczanowska S, Davila E. Ameliorating the tumor microenvironment for antitumor responses through TLR5 ligand-secreting T cells. *Oncoimmunology* 2016; **5**: e1076609.
59 Kantoff PW, Higano CS, Shore ND, Berger ER, Small EJ, Penson DF *et al.* Sipuleucel-T immunotherapy for castration-resistant prostate cancer. *N Engl J Med* 2010; **363**: 411–422.
60 Yoon SI, Kurnasov O, Natarajan V, Hong M, Gudkov AV, Osterman AL *et al.* Structural basis of TLR5-flagellin recognition and signaling. *Science* 2012; **335**: 859–864.
61 Fougere-Deschatrette C, Imaizumi-Scherrer T, Strick-Marchand H, Morosan S, Charneau P, Kremsdorf D *et al.* Plasticity of hepatic cell differentiation: bipotential adult mouse liver clonal cell lines competent to differentiate in vitro and in vivo. *Stem Cells* 2006; **24**: 2098–2109.
62 Krivokrysenko VI, Toshkov IA, Gleiberman AS, Krasnov P, Shyshynova I, Bespalov I *et al.* The Toll-like receptor 5 agonist entolimod mitigates lethal acute radiation syndrome in non-human primates. *PLoS ONE* 2015; **10**: e0135388.
63 Patil SA, Bshara W, Morrison C, Chandrasekaran EV, Matta KL, Neelamegham S. Overexpression of alpha2,3sialyl T-antigen in breast cancer determined by miniaturized glycosyltransferase assays and confirmed using tissue microarray immunohistochemical analysis. *Glycoconjugate J* 2014; **31**: 509–521.

Supplementary Information accompanies this paper on the Oncogene website (http://www.nature.com/onc)